Honda Research Institute EU
Honda Research Institute Europe GmbH
https://www.honda-ri.de/

Evolvable Free-Form Deformation Control Volumes for Evolutionary Design Optimization

Stefan Menzel

2011

Preprint:

This is an accepted article published in Proceedings of the 2011 IEEE Congress on Evolutionary Computation. The final authenticated version is available online at: https://doi.org/10.1109/CEC.2011.5949778

Evolvable Free-Form Deformation Control Volumes for Evolutionary Design Optimization

Stefan Menzel
Honda Research Institute Europe GmbH
Carl-Legien-Str. 30
63073 Offenbach/Main, Germany
Email: stefan.menzel@honda-ri.de

Abstract—**Evolutionary design optimization for improving the performance of real world objects, like e.g. car shapes in the context of aerodynamic efficiency, usually depends on a well-balanced combination of representation, optimizer and design evaluation method. Shape representation requires a fair trade-off between minimum number of design parameters and design flexibility which likewise guarantees a good optimization convergence while allowing manifold design variations. Recently, shape morphing methods have gained increased attention because of their capability to represent complex shapes with a reasonable number of parameters, especially powerful if coupled with numerical simulations for measuring design performance. Free-form deformation, as prominent shape morphing representative, relies on an initial grid of control points, the control volume, which allows the modification of the embedded shape. The set-up of the control volume is a crucial process which in practice is done manually based on the experience of the human user. Here, a method for the automated construction of control volumes is suggested based on a proposed measure E_{CV} which relies on the concept of evolvability as a potential capacity of representations to produce successful designs in a reasonable time. It is shown for target shape matching experiments that optimizations based on E_{CV}-tuned control volumes provide a significantly better performance in design optimization.**

Keywords-evolvability, robustness, free-form deformation, control volume, evolutionary design optimization

I. INTRODUCTION

Shape design optimization addresses, generally spoken, the process of improving the performance of a physical object by the modification of a geometric entity. Hence, a successful computational design optimization is closely coupled to the efficient interplay of three major ingredients: (i) shape representation, (ii) optimization algorithm and (iii) evaluation method for measuring the design performance. With respect to the representation the number and distribution of descriptive shape parameters has to be chosen carefully since both effect strongly design flexibility as well as the convergence time of the optimization algorithm. Typically, a larger number of shape parameters increases possible geometric variations but at the same time it also increases the convergence time of the optimization algorithm due to the larger search space. Recently, shape deformation algorithms have been applied to allow fully automated optimizations of complex shapes [1], especially if combined with numerical simulations for the performance evaluation of design proposals [2, 3, 4]. In contrast to traditional representations, like e.g. NURBS, deformation algorithms do not represent the actual shape but changes to a baseline shape. These changes are realized by a modification of a lattice of control points, the so-called control volume, in which the baseline shape is embedded. By varying the positions of single or groups of control points the shape deformations are realized. In evolutionary design optimization these variations are the encodings referred to as genotype whereas the modified shape which is realized by the deformations is referred to as phenotype.

The set-up of the control volume is usually a manual process and depends strongly on the experience of the human user. Nevertheless, since the initial control volume layout, or in short the control volume, influences the design variation possibilities, the position of each control point has to be chosen carefully. In the present paper, a method is proposed to support an automated control volume set-up process. Based on this method an initial control volume for a free-form deformation (FFD) representation is generated which provides a promising starting point for an efficient optimization. As a prerequisite for this method a measure needs to be defined which quantifies the quality of different control volumes. In the proposed method, this measure is based on the concept of evolvability. Here, the term evolvability refers to the characteristic of a system to provide a fair relationship between a many-to-one genotype-phenotype mapping and phenotype variability. Based on the evolvability criteria FFD control volumes are suggested which are used as starting points for evolutionary design optimizations.

The paper is organized as follows. In section II, FFD as prominent state-of-the-art deformation algorithm is introduced as representation in the area of design optimization. The derivation of the evolvability measure which is utilized for the quantification of FFD control volumes is explained in detail in section III followed by the discussion of experimental results in section IV. Section V summarizes the paper and provides concluding remarks.

II. FREE FORM DEFORMATION IN DESIGN OPTIMIZATION

The choice of an adequate representation plays a rudimentary role in any kind of optimization since it strongly

influences the design variability as well as convergence behavior of the optimization algorithm. In the context of a fully automated design optimization, FFD techniques have proven their efficiency since they are capable to handle shapes of arbitrary complexity. They are especially attractive for the optimization of designs which contain structural inconsistencies like e.g. holes or sharp edges and provide additional advantages as the number of optimization parameters is, generally spoken, arbitrary, i.e. user dependent. Especially if an integration of numerical methods for the quantification of the design performance is required, like e.g. Computational Fluid Dynamics (CFD) simulation for aerodynamic problems, FFD unfolds to a very powerful representation [2, 3, 4].

FFD has been introduced in the late 1980's in the field of computer graphics [5, 6] and is based on spline mathematics. The basic idea behind FFD is depicted in Fig. 1. The sphere represents the object which is the target of the optimization, here given in a triangulated mesh format. It is embedded in a control volume which is defined by a lattice of control points (CP) as well as knot vectors for each spatial dimension. Based on the given control volume the x, y, z-coordinates of the object, i.e. the edges of each triangle, are mapped to the coordinates in the spline parameter space. If the object is a surface point cloud of the design or a mesh which originates from an aerodynamic computer simulation, each grid point within the control volume has to be converted into spline parameter space to allow the deformations. After this process of 'freezing', the object can be modified by moving one control point or several control points to new positions. These new control point positions are taken as inputs for the underlying spline equations and the updated geometry is calculated.

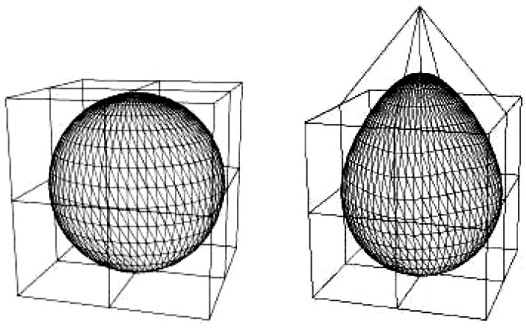

Figure 1. Free-form deformation (FFD), taken from [4].

In case of problems that require finite element or finite volume methods for the numerical analysis in the design evaluation step of an optimization like e.g. for computational fluid dynamics (CFD) or finite element analysis (FEA) problems, FFD has another strong advantage [1, 2, 4]. The fidelity of CFD/FEA simulations depends to a large degree on the quality of the mesh or grid that is used for the numerical simulation. For complex shapes and structures, mesh generation is a very time consuming process (several days), which more often than not requires manual fine-tuning or resolution of meshing problems. In particular, in the context of population based search methods like evolutionary algorithms, manual mesh generation is not feasible. In the FFD framework, the mesh is deformed just like the design is deformed. Therefore, the mathematical deformation procedure is applied to the design and to the mesh simultaneously. This has the huge advantage that mesh generation just has to be done once at the beginning of the optimization for the baseline design. Since everything within the control volume is deformed, a grid from CFD/FEA that is attached to the shape is also adapted. Hence, the deformation affects not only the shape of the design but also the grid points of the computational mesh, which is needed for the CFD/FEA evaluations of the proposed designs. The new shape and the corresponding CFD/FEA mesh are generated at the same time without the need for an automated or manual re-meshing procedure. This feature significantly reduces the computational costs and allows a high degree of automation. Thus, by applying FFD the grid point coordinates are changed but the grid structure is kept. In practice, the complexity of such problems requires a thorough set-up of meaningful control volumes to take problem dimension, design sensitivities as well as design or numerical mesh constraints into account for a successful optimization.

With respect to a typical evolutionary design optimization two steps have to be considered which are important for the method proposed in this paper. In the first step, the preprocessing step, a meaningful control volume has to be generated according to the given shape. In the second step, the actual optimization loop, the shape is optimized based on the control volume which has been generated in the preprocessing step. For visualization reasons, in the present paper the visual shape of an object (and not the CFD/FEA mesh) is the focus. Nevertheless, for numerical grids the idea is straightforwardly applicable. As already mentioned above, the parameter set and consequently the difficulty of the optimization problem can be tuned by the number and selection of control points or control point groups. When defining the parameter set of an FFD system, an optimal trade-off between search space dimension and design flexibility, i.e. freedom of variation, has to be found. However, compared to spline based representations, in the FFD framework the complexity of design variations and not of the initial design is the limiting factor. Therefore, the choice of the number and the positions of initial control points is a crucial question for the design optimization. Usually, it is purely based on the experience of the human user. For the automated way of calculating the initial distribution of control points in the preprocessing step, different control volume layouts have to be compared using a measure for the quantification of the quality of single control volumes. This measure relies on the concept of evolvability and is explained in more detail in section III.

III. On the Evolvability of FFD Control Volumes

In this section, a measure is introduced which quantifies the quality of a single FFD control volume. Based on this measure it is afterwards possible to apply an optimization algorithm which allows an automated calculation of initial control volumes as preferred starting points for the following design optimization. The proposed measure is motivated by the concept of robustness and evolvability of biological systems which is believed to have played a central role in shaping biological diversity and complexity [7, 8]. In this paper, evolvability is considered in the sense of the capacity of a

system to produce favorable phenotypic variations of a design within a moderate number of generations while avoiding non-feasible mutations. A more detailed derivation of an algorithm for measuring the quality of an FFD control volume is based on the distinction between the genotype level, i.e. the encoding, representation or sequence, and the phenotype level, i.e. the system structure, as proposed in [8] to solve the paradox of system robustness and evolvability for biological systems.

Having this genotype-phenotype distinction in mind, it is shown in [8] for biological systems that a representation which generates highly robust structures promotes evolvability. For the RNA genotypes and phenotypes analyzed in [8] the reasons are given by the larger number of neutral networks which are associated with robust phenotypes and the different structures which can be evolved from neighboring samples within the neutral network [8]. The term neutral network describes a collectivity of different genotypes which encode the same/similar phenotype, i.e. a many-to-one genotype-phenotype mapping. Both criteria are utilized for the derivation of the proposed measure for quantifying the quality of FFD control volumes.

A. Set-up of FFD Control Volumes

For simplification but without losing the generalization capability of the proposed method to higher dimensional FFD systems, in the present paper a one-dimensional FFD system is considered. In Fig. 2 a 3D FFD control volume is depicted which consists of a lattice of 4x4x4 control points. One row of 4 control points is extracted neglecting the influence of the y- and z-direction and is discussed in more detail.

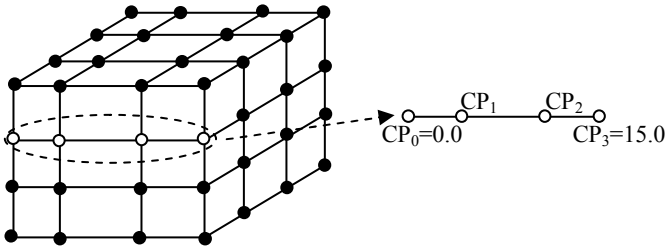

Figure 2. Simplified FFD control volume.

Since FFD relies on splines, most usually B-splines, control volumes are defined by a spline degree, a set of control points and knot vectors [9]. The one dimensional 'control volume' which is analyzed in this paper consists of a clamped B-spline of degree p=3 which is defined by 4 control points CP_0, CP_1, CP_2 and CP_3, i.e. n=3, and a clamped knot vector U chosen to the sequence $[u_0, u_1, u_2, u_3, u_4, u_5, u_6, u_7]=[0, 0, 0, 0, 1, 1, 1, 1]$. CP_0 and CP_3 are always kept fix at x=0.0 and x=15.0 respectively. In practice, the assumption to keep the first and last control point fix corresponds to the fact that it is usually quite straightforward for a human user to determine the values for the minimum and maximum extension of a control volume. The more difficult task is where to place the inner control points to achieve the optimal control volume.

Based on suggested positions for CP_1 and CP_2, the Cartesian coordinates C of a spline are computed according to [9] using the spline parameter $u \in [0,1]$ and the B-spline basis functions given by

$$C(u) = \sum_{i=0}^{n} N_{i,p}(u) CP_i \qquad 0 \le u \le 1 \tag{1}$$

where $N_{i,p}$ is recursively calculated by

$$N_{i,p}(u) = \frac{u - u_i}{u_{i+p} - u_i} N_{i,p-1}(u) + \frac{u_{i+p+1} - u}{u_{i+p+1} - u_{i+1}} N_{i+1,p-1}(u) \tag{2}$$

$$N_{i,0}(u) = \begin{cases} 1 & \text{if } u_i \le u < u_{i+1} \\ 0 & \text{otherwise} \end{cases}. \tag{3}$$

As mentioned above the optimal positions of CP_1 and CP_2 are unknown before an optimization and are usually chosen relying on human experience. Typically, one or more points or regions of interest on the design are focused and control points are placed close to these points or regions. During a manual test the positions are then adapted and refined in a process of selecting and moving control points while observing their influence on the design. In the present paper, these positions will be computed automatically based on a measure E_{CV} which is calculated as a combination of (i) structural robustness S_{CV} and (ii) design variability V_{CV}.

B. Structural Robustness

To initiate the calculation of the evolvability E_{CV} of an FFD control volume a point or region of interest on the design has to be chosen. These points or regions can be based on design features which the human user regards as important for the optimization or, alternatively, on the results of data mining processes of similar designs which e.g. extract sensitive regions of designs using former optimization runs. In the present paper for illustrative reasons one single point of interest POI_x is chosen as a typical representative. For the introductory example the point of interest $POI_{7.5}$ or reference design is given at x=7.5 which results in the FFD system depicted in Fig. 3. The exact positions of CP_1 and CP_2 are unknown.

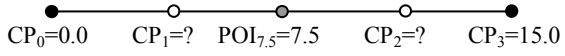

Figure 3. One dimensional FFD $CV_{CP1,CP2}$, $POI_{7.5}$ at x=7.5.

For computing the structural robustness S_{CV} for one chosen control volume CV, the process is as follows. First, both control points CP_1 and CP_2 are set within a range of $CP_0 \le CP1$, $CP_2 \le CP_3$. As an example, CP_1 is chosen to x=1.1 and CP_2 to x=2.2 as depicted in Fig. 4. The base control volume is denoted by $CV_{1.1,2.2}$. Next, the spline coordinate of $POI_{7.5}$ is calculated for the given set-up using the knot vector U by a 'freezing' algorithm, e.g. according to [9]. In the present example, the spline coordinate is $u_{7.5}=0.7538$.

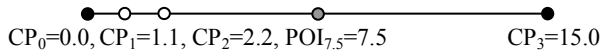

Figure 4. One dimensional FFD $CV_{1.1,2.2}$, CP_1 at x=1.1, CP_2 at x=2.2.

To evaluate the structural robustness S_{CV} for the given control volume, in the next step, the control points CP_1 and CP_2 are varied to all possible positions between CP_0 and CP_3. For each modification, the x-coordinate of $POI_{7.5}$ is updated using (1), (2) and (3) to $POI^*_{7.5}$ and compared to the initial position at x=7.5. If the distance d_{POI} between $POI^*_{7.5}$ and $POI_{7.5}$ is lower than a given threshold, the structural robustness S_{CV} is increased by 1. As an illustrative example, CP_1^* has been moved to 3.1 and CP_2^* to 5.2 respectively. The result for $POI_{7.5}^*$=9.03 is shown in Fig. 5.

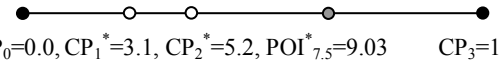

Figure 5. One dimensional FFD $CV_{1.1,2.2}$, CP_1^*=3.1, CP_2^*=5.2.

Pseudocode for the one-dimensional control volume is summarized in Algorithm 1. It is straightforward to extend it to higher spatial dimensions, a larger number of CPs or alternative knot vectors, e.g. knot vectors for unclamped splines.

Algorithm 1. Pseudocode for structural robustness S_{CV}

(a) Determine maximum control volume extensions for CP_0 and CP_3.

(b) Set CP_1 and CP_2 in the range between CP_0 and CP_3.

(c) Select POI and freeze POI using the control volume defined by CP_0, CP_1, CP_2 and CP_3.

(d) Repeat for all possible control point positions CP_1 and CP_2 in the range between CP_0 and CP_3:

- (d1) Move CP_1 and CP_2.
- (d2) Update coordinates of POI to POI^*.
- (d3) Calculate Euclidean distance d_{POI} between POI and POI^*.
- (d4) Increase S_{CV} by 1 if d_{POI} is smaller then a given threshold ε.

(e) Assign structural robustness S_{CV} to chosen control volume.

The idea behind Algorithm 1 is to apply all possible permutations on the control points for a chosen initial control volume and to calculate how many variations of the genotype, i.e. control point positions, produce a similar phenotype, i.e. POI^* position, compared to the initial phenotype. Thus, following the arguments of [8], control volumes with a higher structural robustness S_{CV} would provide a higher evolvability. This argument is supported for FFD in combination with evolutionary optimization. Control volumes with a high structural robustness provide a higher probability for successful mutations because the probability for mutated offspring which achieve at least a similar performance index compared to their parent(s) is higher.

The result of Algorithm 1 for the control volume $CV_{1.1,2.2}$ depicted in Fig. 4 is plotted in Fig. 6. Because of the continuous character of B-splines a discrete sampling step size of 0.5 is introduced for the calculation of a full sampling of the permutations of the control points. A black dot marks the control point positions which produce a distance d_{POI} between POI^* and POI which is within a chosen threshold ε of 0.1, i.e. all control point permutations which generate a POI^* variation below ε are counted as similar. Additionally, only the upper triangle has been calculated. As a remark, considering only the upper triangle has the consequence that the control point order is kept, i.e. $CP_1 < CP_2$, which is important for optimizations which require CFD evaluations to determine the performance index [1]. The structural robustness S_{CV} for control volume $CV_{1.1,2.2}$ as depicted in Fig. 4 is finally computed by the sum of all black dots, thus S_{CV}=4.

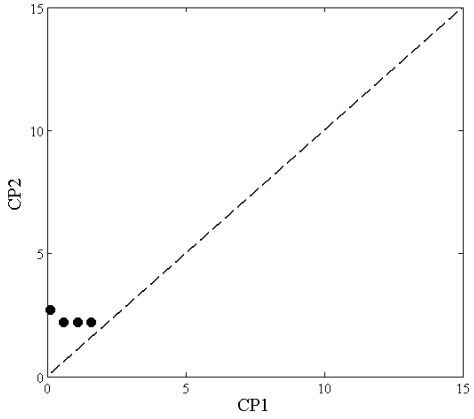

Figure 6. Structural robustness for a control volume $CV_{1.1,2.2}$ shown in Fig. 4.

In a second example, CP_1 is chosen to x=7.1 and CP_2 to x=8.2 as depicted in Fig. 7.

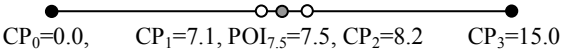

Figure 7. One dimensional FFD $CV_{7.1,8.2}$, CP_1 at x=7.1, CP_2 at x=8.2.

The structural robustness S_{CV} for control volume $CV_{7.1,8.2}$ is calculated to S_{CV}=16 as shown in Fig. 8. Hence, according to structural robustness the potential evolvability of $CV_{7.1,8.2}$ is significantly higher if compared to $CV_{1.1.2.2}$.

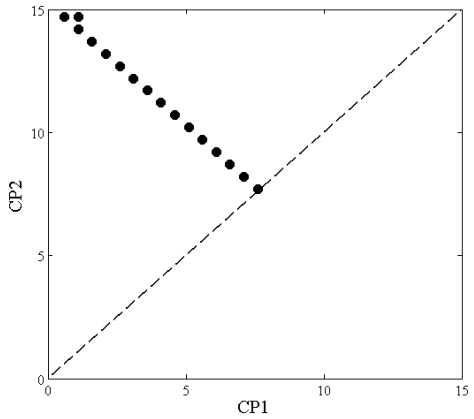

Figure 8. Structural robustness for control volume $CV_{7.1,8.2}$ shown in Fig. 7.

So far, an algorithm has been derived for the calculation of the structural robustness S_{CV} of a *single* base control volume $CV_{CP1,CP2}$. This measure is used to compare different control point settings to find the optimal position of each control point.

For the search of the optimal positions, different strategies are applicable which become especially important for a higher number of control points n since the time complexity depending on sampling intervals m is given by $T=O(m^n)$ for a full sampling. These strategies range within e.g. random sampling, latin hypercube sampling or local/global optimization methods. With respect to an optimization algorithm the encoding is based on the control point x-coordinates of CP_1 and CP_2 as parameter set. If e.g. an evolutionary algorithm is used, the positions are varied by the mutation operator and each proposed control volume is evaluated according to Algorithm 1. An advantage of an optimization algorithm is the possibility to include various constraints, e.g. a required minimum distance between control points or fixed positions of control points. Additionally, if several points of interest POI have to be taken into account, the optimization can be carried out on multiple objectives.

To illustrate the results for the system depicted in Fig. 3 given a $POI_{7.5}$=7.5, a full sampling has been applied, i.e. all possible control point settings have been generated and for each initial control point set-up the structural robustness S_{CV} has been calculated resulting in Fig. 9. The incremental sampling step size has been chosen to 0.5. The black boxes denote the S_{CV} values for CP_1=1.1, CP_2=2.2 and CP_1=7.1, CP_2=8.2 respectively as calculated above by each sum of black dots in Fig. 6 and Fig. 8. As it is clearly visible, the region containing the dark dots refers to the control volume set-ups providing the highest structural robustness. Note: $CP_1 < CP_2$.

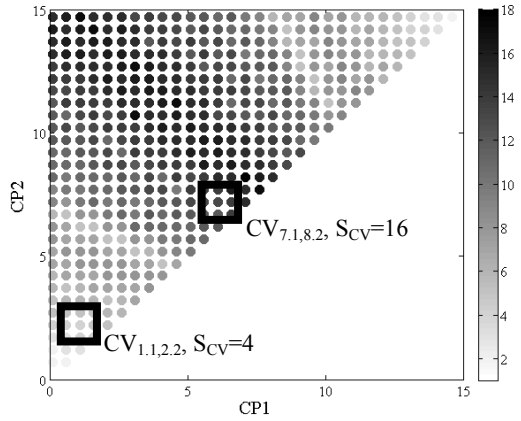

Figure 9. Structural robustness S_{CV} of control volumes for $POI_{7.5}$.

To analyze the influence of different sampling step sizes, the full sampling has been repeated using alternative values. In Fig. 10 the result for a sampling step size of 0.2 is plotted. It is visible that the refinement produces a similar qualitative result. Because of the finer sampling, S_{CV} is higher on absolute values but indicate the same region for optimal control point positions. Nevertheless, choosing a too fine grained sampling strongly increases the computational time. One possible idea in the context of evolutionary optimization would be to choose the sampling step size in close relationship to the expected range of mutations. In the present paper, from the experience of different experiments a sampling step size of maximal 5% of the control volume extension is suggested to achieve a reasonable quality for the structural robustness calculation.

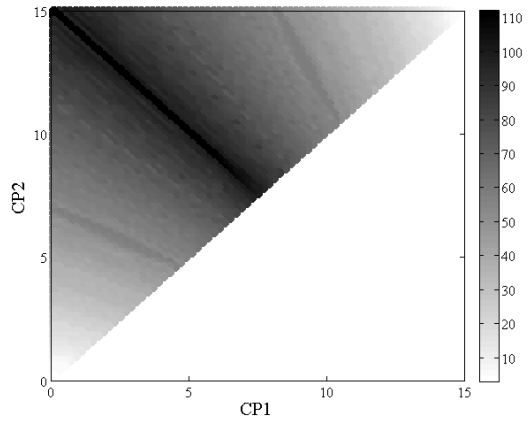

Figure 10. Structural robustness S_{CV} of control volumes for $POI_{7.5}$.

As a second example to visualize the influence of the point of interest on the structural robustness, $POI_{1.0}$ has been chosen to x=1.0 depicted in Fig. 11. The exact positions of CP_1 and CP_2 are unknown.

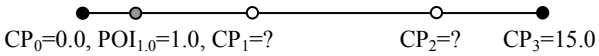

Figure 11. One dimensional FFD $CV_{CP1,CP2}$, $POI_{1.0}$ at x=1.0.

Repeating the steps described above for $POI_{7.5}$ allows the calculation of S_{CV} for $POI_{1.0}$. The result is shown in Fig. 12. It is clearly visible that the region to choose meaningful positions for the control points is broader if compared to $POI_{7.5}$.

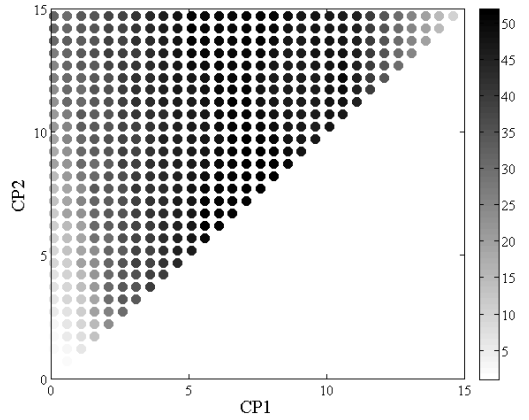

Figure 12. Structural robustness S_{CV} of control volumes for $POI_{1.0}$.

C. Design/Phenotype Variability

Summarizing, so far an algorithm for the calculation of the structural robustness of control volumes has been proposed. To refine the method, design or phenotype variability is considered. Design variability as a second ingredient has also been identified in [8] as an important impact factor for the evolvability of biological systems. With respect to FFD, design variability takes the influence of the control points on the selected point(s) of interest into account. Considering the results of the sampled CP_1 and CP_2 positions given in Fig. 12 for $POI_{1.0}$, a chosen control volume set-up $CV_{5,10}$, i.e. CP_1=5

and CP_2=10, provides a similar structural robustness compared to a chosen control volume set-up $CV_{12,14}$, i.e. CP_1=12 and CP_2=14. Nevertheless, the range of variation for $CV_{12,14}$ is much lower. For $CV_{5,10}$ the 'frozen' spline coordinate of $POI_{1.0}$ results to u=0.0667 and for $CV_{12,14}$ to u=0.02844 respectively. For the calculation of the maximum variability, CP_1 and CP_2 are moved simultaneously for both CVs, first, to 0.0 and, second, to 15.0 which define the maximum extensions of the CV. The x-coordinate of $POI_{1.0}$ is updated by FFD to $POI_{1.0}^*$. As shown in Fig. 13 it is possible to deform $POI_{1.0}$ using the $CV_{5,10}$ set-up to a lower boundary of 0.0044 and an upper boundary of 2.8044. Using control volume $CV_{12,14}$, the boundaries are 0.0003 and 1.2440.

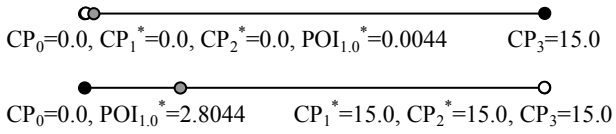

Figure 13. One dimensional FFD $CV_{5,10}$, $POI_{1.0}$.

To calculate the design variability V_{CV} which is assigned to each base control volume the distance between upper and lower boundary is computed and divided by the maximum length, here L=15.0. Thus, the results for $CV_{5,10}$ and $CV_{12,14}$ are $V_{CV5,10}$=(2.8044-0.0044)/15.0=0.1867 and $V_{CV12,14}$=(1.2440-0.0003)/15.0=0.0829 respectively. From these results it is obvious that the design variability using $CV_{5,10}$ is higher than the one of $CV_{12,14}$ which is as expected. Finally, the measure for quantifying the quality of FFD control volumes is the product of S_{CV} and V_{CV} which can be understood as the scaling of S_{CV} on the maximum possible variation calculated by (4). Fig. 9 and Fig. 12 are modified according to (4) and the results for the refined measure E_{CV} are depicted in Fig. 14 and Fig. 15.

$$E_{CV} = S_{CV} \cdot V_{CV} \tag{4}$$

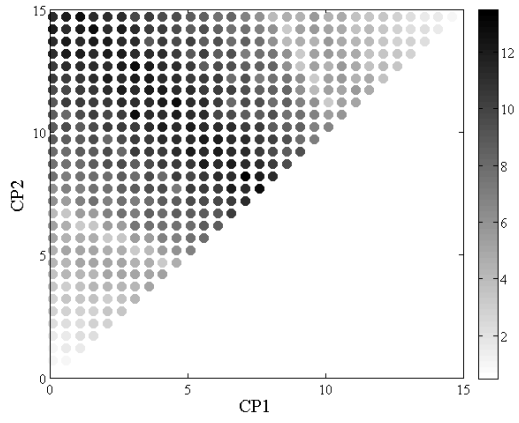

Figure 14. Quality E_{CV} of control volumes $CV_{CP1,CP2}$ for $POI_{7.5}$.

Whereas the difference between E_{CV} and S_{CV} for $POI_{7.5}$ is only minor, the region for meaningful control volumes for $POI_{1.0}$ has changed. The position of CP_2 still has only a minor influence on the quality of the $CV_{CP1,CP2}$ but the impact of the position of CP_1 has increased and should be chosen in a range between 0.1 and 4.0 slightly depending on CP_2.

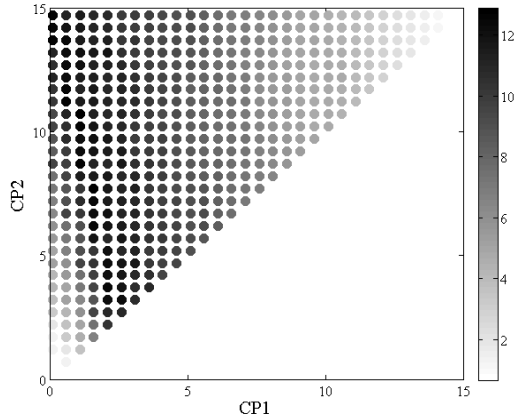

Figure 15. Quality E_{CV} of control volumes $CV_{CP1,CP2}$ for $POI_{1.0}$.

Briefly summarizing, in this section a measure E_{CV} for the evolvability of control volumes has been derived. On the basis of E_{CV} it is possible to compare various control point set-ups and pick a $CV_{CP1,CP2}$ which provides a good starting point for a following design optimization. In the next section, the effect of different control point settings are described in a test scenario.

IV. Experimental Results for Design Optimizations using Evolvable FFD Control Volumes

In this section, experiments are explained which have been carried out to analyze the effects of different control volume set-ups if coupled to an evolutionary design optimization scenario. In this study, the design optimization scenario is based on a shape matching optimization which relies on a one-dimensional FFD system as introduced in section III. The initial or base 'design' is represented by a randomly chosen point of interest within the control volume extensions, thus $0 \leq POI_x \leq 15.0$. The target or optimal 'design' is represented by a randomly chosen single point TP_x within the extensions of the control volume, thus $0 \leq TP_x \leq 15.0$. An example set-up is shown in Fig. 16.

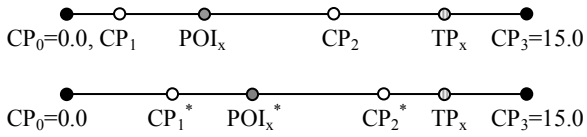

Figure 16. One dimensional FFD CV in shape matching optimization, POI_x and TP_x are chosen randomly.

For a statistical analysis, 1000 optimization runs have been carried out. Each optimization falls into two steps. First, in the preprocessing step two control volumes have been generated which consist of four control points. Since CP_0 and CP_3 are kept fix, CP_1 and CP_2 are chosen randomly for each control volume. Afterwards, the proposed measure E_{CV} is calculated for both control volumes as described in section III using the randomly chosen POI_x. According to E_{CV} both control volumes are sorted into two groups. The control volume with a higher E_{CV} is assigned to group (a) whereas the one with a lower E_{CV} is assigned to group (b). For the target matching optimization, for each experiment the initial control point positions of CP_1 and CP_2 according to (a) or (b) are encoded as parameters into

the genotype. During the optimization run, both positions are varied by the mutation operator of the evolutionary algorithm and utilized to deform the position of POI_x. Hence, the new positions of CP_1^* and CP_2^* are used to compute the updated position of POI_x^*. The design performance f for each design proposal is afterwards computed by the Euclidean distance between POI_x^* and TP_x serving as basis for the selection operator and is calculated by

$$f = \sqrt{(POI_X * - TP_X)^2} \,. \tag{5}$$

The optimization is stopped, i.e. the target point is found, when the distance f is below 0.001. If the target point has not been found within 500 generations the optimization has been terminated and the best fitness recorded. This limit is introduced because test experiments have shown that if the target point TP_x is not matched with a distance of 0.001 within 500 generations the optimizations converged to an optimum which is larger than 0.001. For these runs, it is not possible to find the target point because the FFD setup does not allow a shift of the initial POI_x on TP_x because both control points CP_1 and CP_2 are moved by the optimizer either to 0.0 or 15.0 which are the maximum valid modifications.

For the optimization a standard (1,10)-evolutionary strategy has been implemented [10, 11]. To analyze the effects of the step size adaptation two experimental series have been carried out. In experimental series 1, the mutation operator modifies the parameters using a normal distribution but keeping the mutation step size fixed during the optimization run. In contrast, in experimental series 2 additionally the mutation step size is modified using a log-normal distribution. The initial step size is set to 0.03 for all experiments. For better readability the target matching optimizations (TMO) are labeled as follows:

Exp1(a): 'Exp 1, high E_{CV}', 1st boxplot
TMO based on CVs with a higher E_{CV} w/o step size adaptation

Exp1(b): 'Exp 1, low E_{CV}' , 2nd boxplot
TMO based on CVs with a lower E_{CV} w/o step size adaptation

Exp2(a): 'Exp 2, high E_{CV}' , 3rd boxplot
TMO based on CVs with a higher E_{CV} with step size adaptation

Exp2(b): 'Exp 2, low E_{CV}' , 4th boxplot
TMO based on CVs with a lower E_{CV} with step size adaptation

The overall results are depicted in Fig. 17, Fig. 18 and Fig. 19. In Exp1(a) 54.7 % of all optimizations found the target design (median=81 generations), in Exp1(b) the number drops to 46.2 % (median=499 generations). The integration of the step size adaptation increases the number of matched designs in Exp2(a) to 84.1 % (median=68 generations) and in Exp2(b) to 79.3 % (median=99.5 generations). Both medians of series (a) are significantly (T-test: 5% significance level) better compared to series (b). The fitness value, i.e. the final distance between target design and optimal design, is low for all experiments (median of Exp1(a), Exp2(a) and Exp2(b)≈1e-3, median of Exp1(b)=7e-2). Nevertheless, in Fig. 18 and Fig. 19 it is visible that in both experiments the runs (a) outperform optimization runs (b) with respect to 75th percentile and the most extreme data points (without outliers).

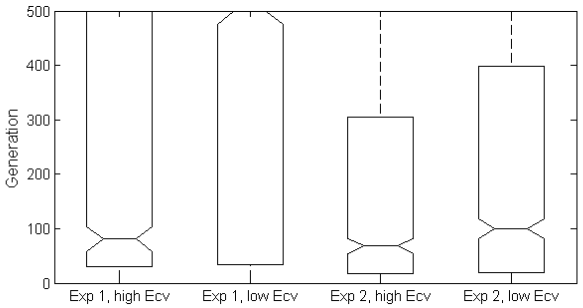

Figure 17. Convergence of target matching optimization.

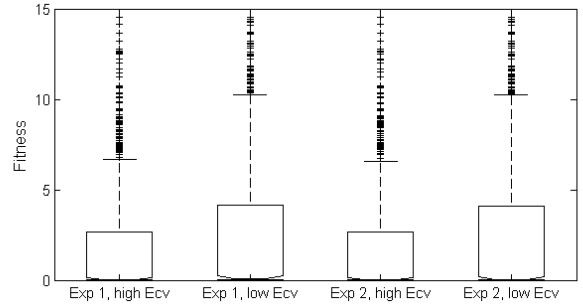

Figure 18. Final distance between optimal and target design.

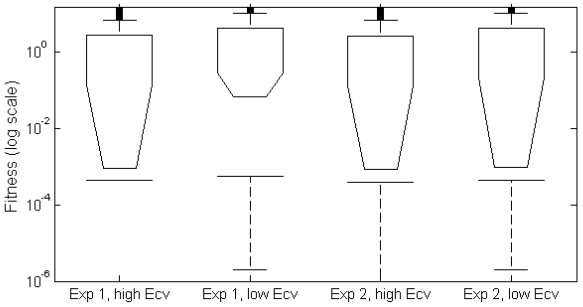

Figure 19. Final distance between optimal and target design (log scale).

For further analysis, a subset of all experiments has been considered consisting of all experiments which did not converge to the target point within 500 generations using (a) and (b). Since it is not possible for these set-ups to find the target point for geometric reasons, it is worth to compare the minimum distances they have achieved. In Exp1, 40 % did not match the target point whereas in Exp2 only 5.4 % failed for both control volumes. The results are depicted in Fig. 20.

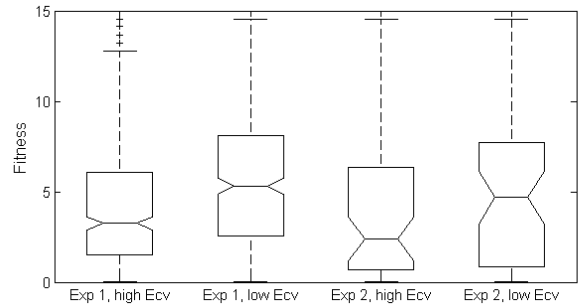

Figure 20. Fitness of non-matched solutions.

The four boxplots shown in Fig. 20 consider the best fitness of each experiment. As it is clearly visible, the fitness values of the optimal designs are much smaller for the runs using control volumes with a higher E_{CV}. For Exp1(a) they are significantly smaller compared to Exp1(b) (T-test: 5% significance level). It should be noted that the step size adaptation has a strong positive effect for optimization convergence.

To evaluate the optimization speed, subsets of the experiments are taken consisting of all optimizations which matched the target point using (a) and (b). In Exp1, 40.9 % found the target point, in Exp2 the number increases to 68.6 %. Based on the generation numbers which reflect the point of time when the target has been found the boxplots depicted in Fig. 21 are calculated. The medians of Exp1(a) and Exp1(b) equal 28 and 30 respectively. In Exp2 the median is 25 for both variants, nevertheless the 75th percentile of Exp2(a) is lower (129) compared to Exp2(b) (173).

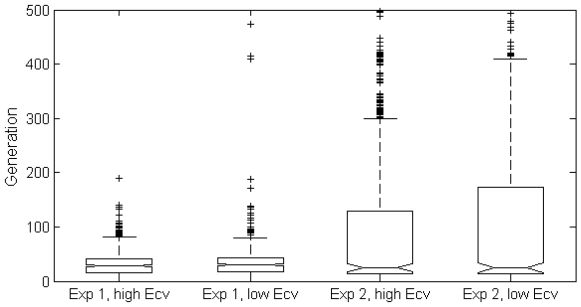

Figure 21. Convergence of matched solutions.

In summary, the experiments underline the efficiency of control volumes with a high evolvability E_{CV}. Optimizations based on these control volumes are faster (Fig. 17 and partly Fig. 21) and provide a better fitness (Fig. 20). An integration of the mutation step size adaptation improves the evolutionary optimizations strongly, nevertheless conserving the positive effects of evolvable control volumes. As a side remark, it is worth noting that the step size adaptation partly reduces the disadvantages of non-favorable control volumes, visible in the reduced gap of matched target designs. The difference decreased from 54.7-46.2=8.5 % to 84.1-79.3=4.8 %.

V. CONCLUSION

Evolutionary design optimizations rely on an efficient interplay between representation, optimization algorithm and evaluation method. In contrast to representations which allow the direct modification of shapes, deformation methods alter designs by the variation of an initially defined control volume which encloses the base design. Usually, the construction of the control volume is a manual process carried out by a human user who decides on number and distribution of control points.

In the present paper, a method is proposed which automates this process by suggesting the application of an optimization algorithm to find the control point positions automatically. As a prerequisite for this optimization a measure is defined which allows a comparison of different control volume layouts. The measure E_{CV} proposed in this paper relies on the concept of evolvability which refers to a system capacity for generating successful design proposals within a reasonable time span. As it has been shown in literature, evolvability is likewise influenced by system robustness and design variability. Both criteria have been transferred to FFD systems. A combination of both, structural robustness S_{CV} and design variability V_{CV}, leads to a measure for evolvability E_{CV} which quantifies the quality of control volumes.

As a consequence, the proposed measure E_{CV} allows an optimization algorithm to find promising initial distributions of control points. In a practical framework, the user identifies one or several points of interest on the design, e.g. according to visible shape features or the results of data mining algorithms, and specifies the maximum extensions of the control volume as well as the number of control points for each spatial dimension. After executing the optimization the optimal control point positions are automatically calculated and suggested to the user as starting control volume for a follow-up design optimization.

For evolutionary design optimization experiments it has been shown that E_{CV}-tuned control volumes provide a higher convergence probability and achieve a better fitness value within a shorter time span. An inclusion of the adaptation of the mutation step size increases the performance while still preserving the advantages of evolvable control volume layouts.

ACKNOWLEDGMENT

The author thanks Bernhard Sendhoff from Honda Research Institute for the very inspiring discussions during the ECoVoL-project.

REFERENCES

[1] S. Menzel, and B. Sendhoff, "Representing the change – Free form deformation for evolutionary design optimization," in *Evolutionary Computation in Practice*, Springer, Berlin, pp. 63-86, 2008.

[2] J. A. Samareh, "Aerodynamic shape optimization based on free-form deformation," in 10th AIAA/ISSMO Multidisciplinary Analysis and Optimization Conference, 2004.

[3] S. Menzel, M. Olhofer, and B. Sendhoff, "Evolutionary design optimization of complex systems integrating Fluent for parallel flow evaluation," in Proceedings of European Automotive CFD Conference, pp. 279-289, Frankfurt, 2005.

[4] E. C. Perry, S. E. Benzley, M. Landon, and R. Johnson, "Shape optimization of fluid flow systems," in Proceedings of ASME FEDSM'00, ASME Fluids Engineering Summer Conference, Boston, 2000.

[5] T. W. Sederberg, and S. R. Parry, "Free-form deformation of solid geometric models," Computer Graphics, 20(4), pp. 151-160, 1986.

[6] S. Coquillart, "Extended free-form deformation: a sculpturing tool for 3D modelling," Computer Graphics, 24(4), pp. 187-196, 1990.

[7] H. Kitano, "Biological robustness," Nature Review Genetics, vol. 5, pp. 826-837, 2004.

[8] A. Wagner, "Robustness and evolvability: a paradox resolved," in Proc. R. Soc. B, vol. 275, pp. 91-100, 2008.

[9] L. Piegl, and W. Tiller, "The NURBS book," Springer, Berlin, 2nd edition, 1997.

[10] T. Bäck, D. B. Fogel, and Z. Michalewicz, "Evolutionary computation," Taylor & Francis, 2000.

[11] H. P. Schwefel, "Evolution and optimum seeking," John Wiley & sons, New York, 1995.